

HEALTH MONITORING OF CARBON NANOTUBE (CNT) HYBRID ADVANCED COMPOSITES FOR SPACE APPLICATIONS

Sunny Wicks⁽¹⁾, Derreck Barber⁽¹⁾, Ajay Raghavan⁽²⁾, Christopher T. Dunn⁽²⁾, Leo Daniel⁽¹⁾, Seth S. Kessler⁽²⁾, Brian L. Wardle⁽¹⁾

⁽¹⁾MIT, Dept. of Aeronautics & Astronautics, 77 Massachusetts Ave., Cambridge, MA 02139, USA,
Corresponding Author: Prof. Brian L. Wardle, wardle@mit.edu, (617) 252-1539

⁽²⁾Metis Design Corporation, Cambridge MA 02141 USA

ABSTRACT

Damage detection in hybrid fiber reinforced composites containing fully-integrated aligned carbon nanotubes (CNTs) in the polymer matrix is reported. Due to unique alignment and distribution of carbon nanotubes (CNTs) through the thickness of the composites, significant interlaminar and intralaminar mechanical property improvements have been observed for these nano-engineered composites, including interlaminar strength and toughness. These materials exhibit high electrical conductivity that is enhanced by many orders of magnitude: 10^6 and 10^8 for the in-plane and through thickness directions, respectively. This inherent multifunctional characteristic is utilized to solve sensing challenges in non-destructive evaluation (NDE) and potentially structural health monitoring (SHM). Impact damage was observed to cause significant resistance changes, which allows for a full-field representation of the damage locations (and perhaps type) by interpolating the collected data via patterned circuits deposited on the laminates. The concomitant increases in mechanical and electrical laminate properties increases the feasibility of introducing multifunctionality of structural health monitoring for space applications.

1. INTRODUCTION

The future of space transportation systems relies on the technical and economical feasibility of reusable launchers. These vehicles require more complex design and technologies in comparison to current launchers, since they have to withstand harsh environmental conditions with improved safety, reliability and cost effectiveness in order to drastically increase the frequency of flights while reducing maintenance efforts in-between flights. To achieve this, the vehicles have more stringent structural requirements, particularly in the area of damage detection and overall structural integrity. One of the key technologies to be developed is that of structural health monitoring, including sensor technologies and non-destructive inspection (NDI)

methods required for in-flight and between-flights monitoring of structural and functional health aspects [1, 2]. Another emerging technology is a space propellant depot, as pictured in Fig 1. This is an affordable, near-term depot that utilizes existing and in development technologies to provide passive low to zero-boil-off cryogenic propellant storage [3]. Such a depot will require a high level fidelity of structural health monitoring, particularly in the LOX/LH2 tanks. This is important in order to minimize maintenance and refurbishment operations and to extend components lifetime. It has been reported that up to 27% of a commercial aircraft's life cycle cost is due to inspection and maintenance. Therefore, since the cost for maintaining a fleet of spacecraft can be considerably higher than for aircraft, the importance of inspection and maintenance reduction is evident.

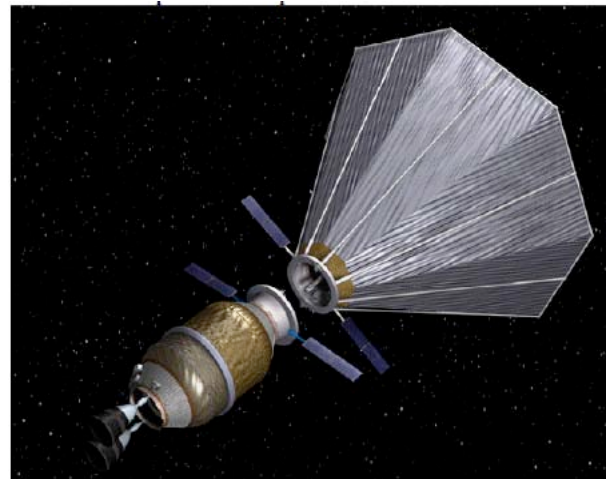


Fig. 1. Propellant depot that enables orbital refueling supporting exploration, science, and other space endeavors [3].

Current research into nano-engineered composites has yielded materials with vastly improved electrical conductivity vs. composites without CNTs, such that it may be possible in some applications to substitute metals with FRP nano-composites (with the

incorporation of carbon nanotubes (CNTs) into the polymer matrix) [4-7]. This new approach also has the potential multifunctional aspect of damage sensing which is explored here.

1.1 SHM Concept Overview

Recent efforts to address the limitations of advanced composites include the incorporation of carbon nanotubes (CNTs) into the polymer matrix of the composite. Exceptional physical properties of CNTs including mechanical stiffness (as high as 1 TPa in some experiments [8]) and electrical conductivity (~1000x copper under certain conditions) make them an attractive constituent in traditional composites [9]. Capturing these nanoscale properties in a macroscale material presents many challenges: issues with dispersion, alignment and feasible volume fraction of the CNTs limit bulk property improvements. The work presented in this paper assesses the feasibility of using enhanced electrical conductivity in a structural health monitoring concept.

Nano-engineered composites allow control of the location and direction of CNTs to optimize reinforcement directions. In prior work, CNTs are arranged radially on the surfaces of advanced fibers and infiltrated with epoxy to create ‘fuzzy-fiber’ reinforced plastics (FFRP) [10, 11], as shown in Fig. 2. The use of CNTs serves a multi-faceted purpose: while reinforcing matrix regions between fibers and between plies is the primary objective, secondarily, percolating conductive networks are created that vastly improve conductivity of the bulk composite material. Past work indicates a significant ($10^6 - 10^8$) increase of electrical conductivity of alumina-fiber based FFRP, as shown in Fig. 3 as a function of CNT volume fraction. Such enhanced conductivity enables advanced structural health monitoring techniques that may detect internal damage before it can be visually identified.

‘Fuzzy-Fiber’ FFRP hybrid composite

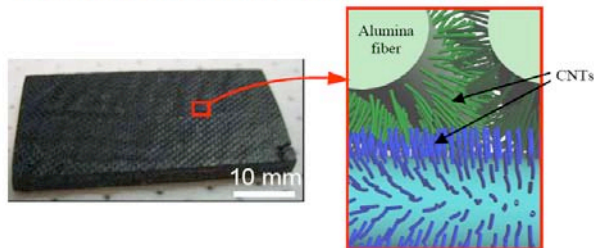


Fig. 2. FFRP laminate composed of cloth containing alumina fibers (in tow form) with *in situ*-grown aligned CNTs in a polymer matrix (left), and illustration of cross-sectional region between tows (right) [12].

Structural health monitoring (SHM) has been established as a route to assess the level of damage in a composite without relying on visual inspection. CNT-enhanced composites show promise to improve the conductivity of composites allowing for monitoring systems that can measure changes in resistance in real time to discover local damage before catastrophic failure [1, 2]. Thostenson and Chou built CNT-enhanced advanced fiber-reinforced composites with improvements in electrical conductivity and had encouraging results in damage monitoring using passive in-plane electrical resistance measurements [13]. However, their approach to incorporating CNTs in the fiber-reinforced composite results in random alignment of short and very low volume fraction CNTs, resulting in no significant improvement in mechanical properties. Further, their approach to SHM used *in-plane* resistance measurements that would require a dense network of invasive wiring and instrumentation for practical large-area monitoring. Thus, a refined approach to incorporating CNTs in fiber-reinforced aerospace structural composites for SHM is implemented here, whereby all the potential advantages of CNTs are used for improving mechanical properties as well as enabling SHM with a less invasive electrode network.

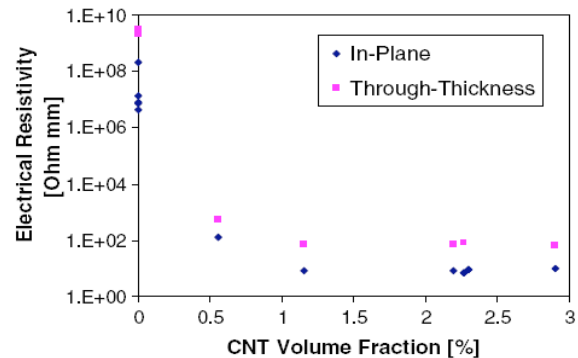


Fig. 3. Electrical resistivity of FFRP for in-plane and through-thickness directions vs. CNT volume fraction [4].

2. EXPERIMENTATION

In this section, the synthesis of CNTs and the manufacturing process of baseline (no CNTs) and FFRP (with CNTs) laminates are described, as well as sensor testing protocols.

2.1 Sample Manufacturing

Composite samples are fabricated using a woven alumina ceramic cloth. Aligned CNTs are grown using chemical vapor deposition (CVD) [14]. As-manufactured alumina cloth is dipped in a 50mM solution of isopropanol and iron nitrate, coating

individual fibers (intra-tow) with the iron catalyst including those inside every tow. The dip-coated cloth is dried in ambient air then placed in a tube furnace. The system is heated in a hydrogen environment that reduces the catalyst on the surface of the fibers into iron nanoparticles. Ethylene gas is then introduced, which decomposes and reacts with the catalyst particle to grow aligned carbon nanotube forests. The CNTs extend perpendicular to the fiber surface and bridge neighboring fibers and plies [15], as depicted in Fig. 2. The CNTs are typically longer than the spacing between the composite plies ($\sim 10\ \mu\text{m}$) and between the fibers ($\sim 1\text{-}5\ \mu\text{m}$). A fuzzy-fiber ply and laminate are shown in Fig. 4.

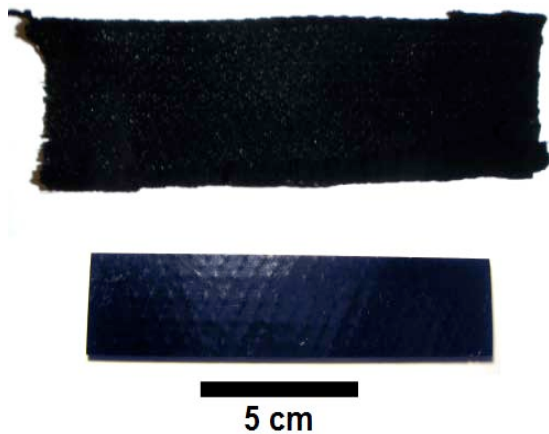


Fig. 4. A fuzzy fiber ply (top) and FFRP laminate (bottom) [6].

Both the baseline and FFRP specimens were manufactured to be two plies thick using hand lay-up, following the procedure illustrated in Fig. 5. Each cloth layer is placed on a sheet of guaranteed non-porous Teflon (GNPT) and coated in West Systems epoxy (Resin 105 and Hardener 206). The epoxy is wicked into the interior of the woven ply within a few seconds, after which another ply is placed on top and coating repeated. The aligned CNT forests assist with wetting the ply, as it has been shown that *aligned* CNT forests wet easily and draw epoxy into the forest by strong capillary action [16]. After the laminate is created, porous Teflon (PT), absorbent bleeder paper, and GNPT are placed over the laminate. A caul plate and vacuum are then used to provide pressure to the assembly and ensure uniform thickness. After curing for at least 12 hours, the sample is trimmed with a diamond-grit cutting wheel.

2.2 Experimental Testing

Enhancement of structural health monitoring enabled by the increase in laminate conductivity due to aligned

CNTs is studied using previously developed SHM procedures. A non-invasive silver-ink electrode grid and multiplexing micro-switches will be connected to compact hardware for through-thickness resistance measurements in the full implementation. Here, a silver ink painted electrode grid, inspired by flat panel liquid crystal display (LCD) technology, creates an “active” layer of electrode columns on one surface of the laminate as a positive electrode, and on the other surface another layer of electrode rows will act as “passive” ground (see Fig. 6). By cycling through particular row and column selections, local through-thickness resistance measurements can be obtained for a grid of points over the structure, in addition to in-plane data. In the current implementation, multiplexing is not used but rather manual point-wise stepping of electrical grid points.

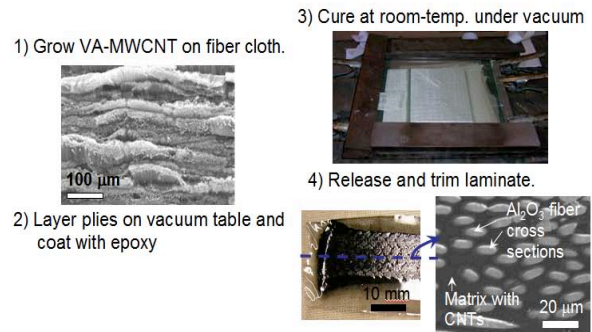


Fig. 5. Hand lay-up procedure used to fabricate all laminates in this work [6].

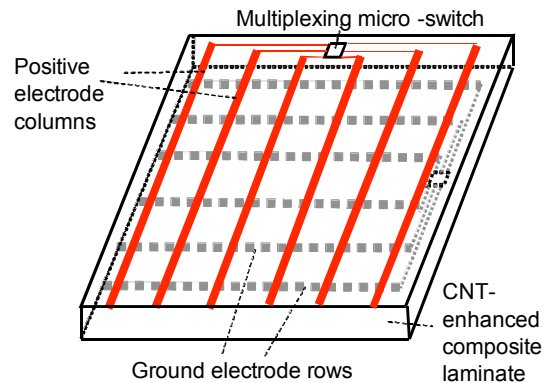


Fig. 6. Silver ink electrode and multiplexing switch for through-thickness and in-plane conductivity measurements [5].

Structural damage in the form of delamination and cracks affect local through-thickness (and in-plane) resistance, especially for CNT-enhanced specimens where a percolating CNT network is created. By interpolating between measurements at distinct grid points with the electrode network, high-resolution

through-thickness electrical-resistance-change maps over large structural areas may be obtained, allowing for accurate localization of damage. Using through-thickness resistance from non-invasive techniques as the monitoring parameter allows for easy scaling with low mass and space penalty, which is crucial in space applications. Because secondary considerations such as static mechanical load and hysteresis effects affect resistance measurements, results must be carefully examined to distinguish damage from these other factors [17].

Two specimen groups were fabricated: baseline and FFRP specimens. A complete test matrix of 3 baseline and 8 FFRP specimens have been manufactured using this technique. The baseline laminates have dimensions of 4.5 x 1 x 0.08 in (114 x 25 x 2 mm), while the FFRP samples have dimensions of 4.5 x 1 x 0.12 in (114 x 25 x 2 mm). On the top surface, 22 parallel conductors were patterned in the short-dimension, and 4 parallel conductors were patterned in the long dimension on the opposite surface as shown in Figures 7 and 8.

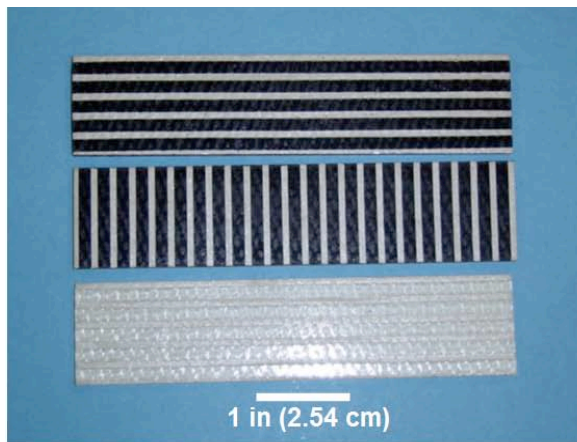


Fig. 7. Two FFRP samples and one baseline sample with silver paint stripe electrodes.

Prior to impact, the resistance of each specimen was measured: 1) between each parallel trace in-plane, and 2) at each grid point created by the intersection of perpendicular top and bottom traces through-thickness. Initial data showed significant variability when probing directly on the silver traces. To address this issue, a procedure was developed that involved bonding thick gauge wire to the traces using silver epoxy, resulting in < 2% change across 10 repeat trials. Each of the specimens (1 baseline and 1 FFRP to date) was impacted with 75 ft-lbs using a guided dropped weight impact device, calibrated to cause minor surface micro-cracking on the composite surface. Following impact, post-damage electrical resistance measurements were collected for each possible grid combination. Optical

microscope images of each specimen were also taken before and after impact in order to document the effects of the impact event on the surface of each specimen.

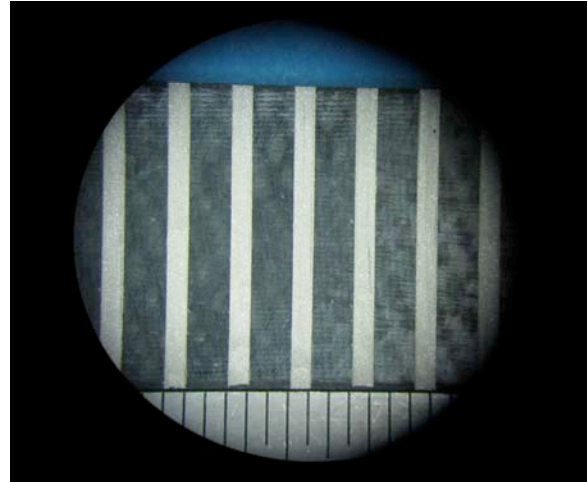


Fig. 8. Image of an electroded FFRP laminate. Tick marks at bottom are 1.6 mm (1/16").

3. RESULTS

Following impact, no damage was visible to the unaided eye for either specimen on either surface. Microscopy, however, revealed cracking on the back surface (opposite from the impact surface) for both the baseline and FFRP laminates (Fig. 9). The extent of damage between the baseline and FFRP specimens remains to be assessed. The original planned experiment had called for an analog multiplexer to switch electrode pairs for ease of measurement, however, due to time constraints the previously described instrumentation process was implemented for the presented results. Two sets of data were collected for the pre- and post-impact damage evaluation: 1) in-plane between each parallel pair of adjacent traces, and 2) through-thickness at each grid point created by the virtual intersection of the perpendicular top and bottom surface traces.

First, for the baseline laminate, all measured values for both in-plane pairs and through-thickness pairs were higher than the range of the multimeter (5 M Ω) before and after impact. It was clearly evident that without the CNT enhancement, there is no suitable conductive path formed for electrical evaluation. Next, data was collected for the in-plane resistance of the FFRP. For the short traces the average resistance is 9 Ω pre-impact. Following impact, while the outermost trace pairs on either side of the damage site along the x-axis showed < 10% change, the middle was consistently > 100%. Only minor changes (< 1%) were detected

between long trace pairs. Finally, electrical resistance data was collected for the 56 through-thickness grid points, which averaged 20Ω pre-impact. As seen in Fig. 10, a clear change of $> 100\%$ was detected in the impacted region. Along the x-axis, between the measurement points for the long traces (left edge in Fig. 10) and the damage site, $< 10\%$ change was observed. However on the opposite side of the damage site (right side of Fig. 10), a constant resistance offset was introduced due to the presence of cracks across the backface electrodes.

It is interesting to note that the results do not show peak changes exactly at the center of the impact target. This may indicate that the parameters are sensitive to different damage modes. For instance, in-plane resistance may be more sensitive to surface cracks, which tend to form at the edge of the impact zone. Conversely, through-thickness resistance may be more sensitive to delamination, which would affect the CNT links across the specimen plies. More extensive testing is required to investigate this further, as has been done in the past for other damage sensing techniques that show different relative sensitivities to different damage modes.

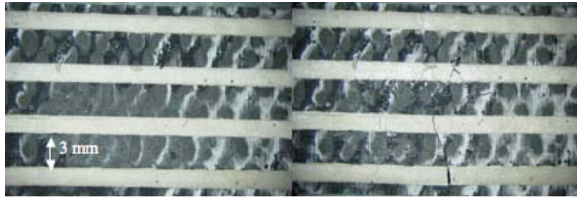


Fig. 9. Before (left) and after (right) photographs of CNT-enhanced specimen impacted on opposite side. Silver lines are spaced approximately 3mm edge-to-edge, and 1.5mm wide [5].

4. CONCLUSIONS

CNT-enhanced laminated FRP composites were fabricated, patterned with a silver ink electrode grid, and subsequently subjected to impact damage. Both in-plane and through-thickness electrical resistance measurements were collected. Clear changes were observed in both sets of data for traces close to the impacted zone of the specimen, demonstrating that these parameters were sensitive to damage in the structure. The peak changes were close to the center of the specimen near the impact site, and there was little to no change in values at points away from the damage zone. Overall, the barely visible impact damage caused significant resistance change, which may allow for a full-field representation of the damage locations by interpolating the collected data. This demonstrates the potential of using this approach as an SHM solution,

with the added benefit of CNT reinforcement of the laminates.

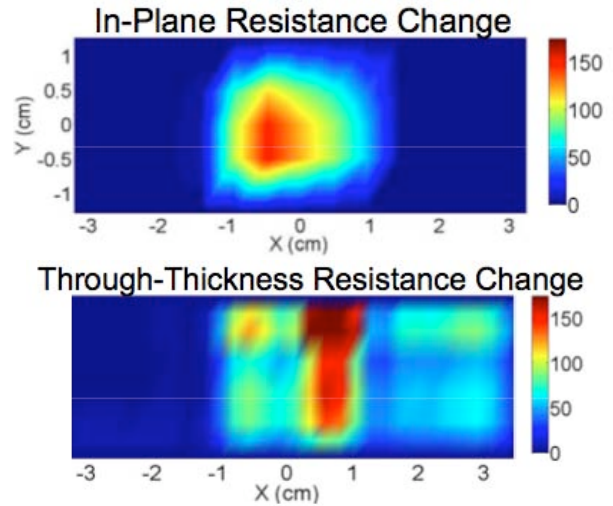


Fig. 10. Representation of in-plane and through-thickness resistance changes after impact. Red indicates largest relative resistance change [5].

Near-term research will aim to further validate this method with additional specimens in a more comprehensive test matrix, as well as to observe the effects of multiple progressive impact events. Furthermore, pre- and post-damage tensile tests will be conducted to evaluate residual strength and stiffness for baseline and FFRP laminates. The multiplexed circuit originally envisioned will be implemented to leverage direct-write technology to create more accurate electrode grid formations.

Future work will focus on facilitating data acquisition with improved hardware, the ultimate goal being to have standard equipment for SHM at the component level. A flexible circuit frame (flex-frame) has been designed as a single double-sided copper-coated-Kapton that will help to eliminate variability in data. Current techniques require half a day per sample due to data acquisition by hand with a multimeter, while the flex-frame system will allow 1140 total measurements to be gathered in one second to one hour, depending upon settling times for data. Alternative SHM schemes like acoustic emission (AE) could also be explored that would use the same flex frame to detect dynamic resistance changes induced by wave perturbations.

5. ACKNOWLEDGMENTS

This research was sponsored by the Air Force Office of Scientific Research (AFOSR) under the Phase I STTR contract FA9550-09-C-0165. The work was performed

at the Metis Design Corporation in Cambridge, MA and at MIT's Department of Aeronautics and Astronautics, in Cambridge, MA. Derreck Barber gratefully acknowledges support from the Paul E. Gray (1954) Endowed Fund for UROP. Materials (FFRP composites) developed with support from Airbus S.A.S., Boeing, Embraer, Lockheed Martin, Saab AB, Sprit AeroSystems, Textron Inc., Composite Systems Technology, and TohoTenax through MIT's Nano-Engineered Composite aerospace Structures (NECST) Consortium.

6. REFERENCES

1. Li C, Thostenson ET, and Chou T-W. Sensors and actuators based on carbon nanotubes and their composites: A review. *Composites Science and Technology* 2008;68(6):1227-1249.
2. Thostenson ET and Chou T-W. Real-time in situ sensing of damage evolution in advanced fiber composites using carbon nanotube networks. *Nanotechnology* 2008;19(21):215713.
3. Kutter BF, Zegler F, O'Neil G, and Pitchford B. A Practical, Affordable Cryogenic Propellant Depot Based on ULA's Flight Experience. AIAA SPACE 2008 Conference & Exposition Proceedings. San Diego, California, 9-11 September 2008.
4. Garcia EJ, Wardle BL, Hart AJ, and Yamamoto N. Fabrication and Multifunctional Properties of a Hybrid Laminate with Aligned Carbon Nanotubes Grown In Situ. *Composites Science and Technology* 2008;68(9):2034-2041.
5. Kessler SS, Barber, D., Wicks, S., Raghavan, A., and B.L. Wardle,. Structural Health Monitoring using Carbon Nanotube (CNT) Enhanced Composites. The 7th International Workshop on Structural Health Monitoring (IWSHM07) Proceedings. Stanford University, Sept. 9-11, 2009.
6. Barber DM, et al. Health Monitoring of Aligned Carbon Nanotube (CNT) Enhanced Composites. 2009 SAMPE Fall Technical Conference Proceedings. Wichita, KS, Oct. 2009.
7. Wicks SS, Guzman de Villoria R, and Wardle BL. Interlaminar and Intralaminar Reinforcement of Composite Laminates with Aligned Carbon Nanotubes. accepted to *Composites Science and Technology*, Sep. 2009.
8. Yu M-F, et al. Strength and Breaking Mechanism of Multiwalled Carbon Nanotubes Under Tensile Load. *Science* 2000;287(5453):637-640.
9. Wei BQ, Vajtai R, and Ajayan PM. Reliability and current carrying capacity of carbon nanotubes. *Applied Physics Letters* 2001;79(8):1172-1174.
10. Garcia EJ, Hart, A.J., Wardle, B.L., and Slocum, A. Fabrication and Testing of Long Carbon Nanotubes Grown on the Surface of Fibers for Hybrid Composites. 47th AIAA/ASME/ASCE/AJS/ASC Structures, Structural Dynamics, and Materials Conference Proceedings. Newport, R.I., May 1-4, 2006.
11. Garcia EJ, Hart JA, and Wardle BL. Long Carbon Nanotubes Grown on the Surface of Fibers for Hybrid Composites. *AIAA Journal* 2008;46(6):1405-1412.
12. Wardle BL, Bello, D., Ahn, K., Yamamoto, N., Guzman de Villoria, R., Hallock, M., Garcia, E.J., and A. John Hart. Particle and Fiber Exposures During Processing of Hybrid Carbon-Nanotube Advanced Composites. 2008 SAMPE Fall Technical Conference Proceedings. Memphis, TN
13. Thostenson ET, Chou, T.-W.,. Carbon Nanotube Networks: Sensing of Distributed Strain and Damage for Life Prediction and Self Healing. *Advanced Materials* 2006;18(21):2837-2841.
14. Yamamoto N, et al. High-yield growth and morphology control of aligned carbon nanotubes on ceramic fibers for multifunctional enhancement of structural composites. *Carbon* 2008.
15. Wicks SS, Guzman de Villoria R, Barber DM, and Wardle BL. Interlaminar Fracture Toughness of a Woven Advanced Composite Reinforced with Aligned Carbon Nanotubes. 50th AIAA/ASME/ASCE/AHS/ASC Structures, Structural Dynamics, and Materials Conference Proceedings. Palm Springs, CA
16. Garcia EJ, Hart AJ, Wardle BL, and Slocum AH. Fabrication of composite microstructures by capillarity-driven wetting of aligned carbon nanotubes with polymers. *Nanotechnology* 2007;18(16):165602.
17. E. T. Thostenson T-WC. Carbon Nanotube Networks: Sensing of Distributed Strain and Damage for Life Prediction and Self Healing. *Advanced Materials* 2006;18(21):2837-2841.